A STUDY ON INDUSTRIAL GAMMA RAY CT WITH A SINGLE SOURCE-DETECTOR PAIR

JONGBUM KIM*, SUNGHEE JUNG and JINSUP KIM
Korea Atomic Energy Research Institute
150 Deokjin-dong, Yuseong-gu, Daejeon, 305-353, Korea
*Corresponding author. E-mail : jong@kaeri.re.kr

Received September 15, 2005
Accepted for Publication January 18, 2006

Having its roots in medical applications, industrial gamma ray CT has opened up new roads for investigating and modeling industrial processes. Using a line of research related to industrial gamma ray CT, the authors set up a system of single source and detector gamma transmission tomography for wood timber and a packed bed phantom. The hardware of the CT system consists of two servo motors, a data logger, a computer, a radiation source and a radiation detector. One motor simultaneously moves the source and the detector for a parallel beam scanning, whereas the other motor rotates the scan table at a preset projection angle. The image is reconstructed from the measured projections by the filtered back projection method. The phantom was designed to simulate a cross section of a packed bed with a void. The radiation source was 20mCi of Cs-137 and the detector was a 1 inch × 1 inch NaI (TI) scintillator shielded by a lead collimator. The experimental gamma ray CT image has sufficient resolution to reveal air holes and the density distribution inside the phantom. The system could possibly be applied to a packed bed column or a pipe flow in a petrochemical plant.

KEYWORDS : Industrial Process Diagnosis, Gamma Ray, Transmission Tomography, Petrochemical Industry, Filtered Back Projection, Image Reconstruction

1. INTRODUCTION

With wide industrial application, computerized tomography (CT) is a rapidly developing technique that is especially useful for imaging and measuring multi-component and multi-phase processes. Tomographic measurements can be obtained by using different sensors, such as X-ray, ultrasonic, optical and microwave sensors, as well as electrical impedance electrodes [6].

X-ray, ultrasonic and microwave sensors are widely used for medical purposes, as are various types of gamma emission CT such as single photon emission computed tomography and positron emission tomography [1]. However, medical tomographic systems seldom use transmission-based gamma-ray CT where the source and detector are located outside of the object.

Unlike medical CT, which is optimized for the human body, industrial CT should be applied to systems of various sizes and densities, depending on the local situation. For the resolution and contrast of a small system, X-ray CT or NDT (Non Destructive Test) film is more useful than gamma ray CT.

Nonetheless, gamma-ray CT has many advantages over X-ray CT or ultrasonic CT in the diagnosis of large-scale industrial process units. As shown in Fig. 1, the mean free path ($1/\mu$) of a material increases as the photon energy increases [3]. This result means that CT with a higher energy gamma ray can produce a good contrast for a large-scale system. Although the resolution of gamma ray CT is lower than that of X-ray CT, even a low resolution image can

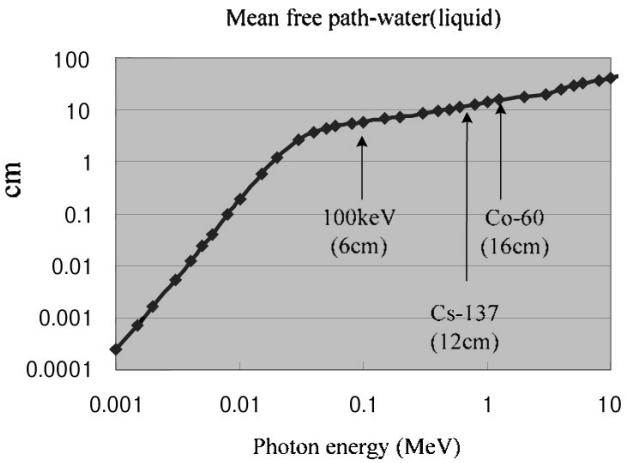

Fig. 1. Mean Free Path vs. Photon Energy in Water

give a plant engineer valuable information. The information may include details of the distribution of a material flow, a blockage, channeling or the location of crystallized coke. Furthermore, a sealed gamma ray source can be easily handled, installed and moved in various local plant environments.

We now present, as a part of our research on industrial CT, the preliminary results from a single source-detector pair system. The results are promising. Our gamma ray CT focuses on an industrial application and the material of the object to be scanned is similar to the inside of a process unit [6].

2. THEORY AND THE MEASUREMENT SYSTEM

2.1 The Principle of Gamma Transmission Tomography

In a gamma-ray transmission, the transmitted intensity, I, of a mono-energetic radiation beam traversing an object of thickness u is given by the following equation:

$$I = I_0 e^{-\int \mu(x,y)du}, \tag{1}$$

Where I_0 is the incident beam intensity of the radiation beam and $\mu(x,y)$ is the linear attenuation coefficient [1]. Equation (1) can be rearranged as follows:

$$In\frac{I_0}{I} = \int \mu(x,y)du\ . \tag{2}$$

The line integral along the path of u is known as the ray-sum. In Fig. 2, P(s,θ) is the line integral of μ(x,y) along a line inclined at an angle θ from the x axis and at a distance s from the point of origin [2]. Mathematically, it is written as follows [1]:

$$p(s,\theta) = \int \mu(x,y)du\ . \tag{3}$$

As a result, the projections are a set of ray-sums at each angle. The projection equation, which is the Radon transformation of μ(x,y), is expressed as follows:

$$p(s,\theta) = R\mu(x,y), \tag{4}$$

Where R is the Radon transform operator [2].

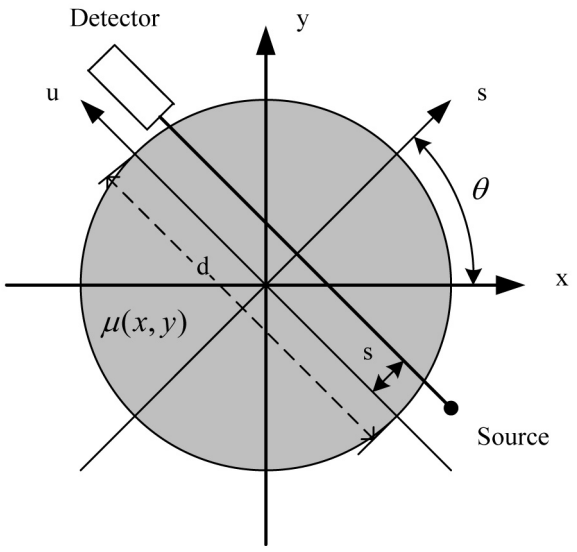

Fig. 2. A Ray-Sum

The radiation intensity is converted to a linear attenuation value as follows:

$$P = \mu = \frac{1}{d}\ln\left(\frac{I_0}{I}\right). \tag{5}$$

2.1.1. The Image Reconstruction Method

The gamma ray CT system introduced here is a first-generation scanning type that uses a one source-detector pair and a parallel beam [6]. The algorithm for the parallel beam is based on the filtered back projection (FBP) method. The FBP method is a well-known classical technique, the algorithm of which is shown in Fig. 3 [2].

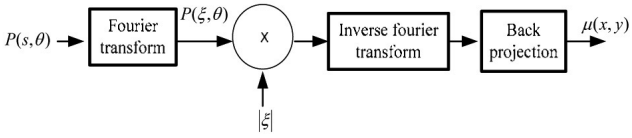

Fig. 3. Filtered Back Projection Routine

In Fig. 3, $p(\xi,\theta)$ denotes the Fourier transform of p(s,θ)

Mathematically, it is written as follows:

$$P(\xi,\theta)=\int_{-\infty}^{\infty} p(s,\theta)\exp(-j2\pi\xi s)ds\,, \tag{6}$$

Where $\hat{p}(s,\theta)$ denotes the inverse Fourier transform of $p(\xi,\theta)\cdot|\xi|$ [2]. Mathematically, it is written as follows [2]:

$$\hat{p}(s,\theta)=\int_{-\infty}^{\infty}|\xi|P(\xi,\theta)\exp j2\pi\xi s d\xi\,. \tag{7}$$

The reconstructed image can be obtained from a back projection of $\hat{p}(s,\theta)$. That is,

$$\mu(x,y)=\int_{0}^{\pi}\hat{p}(x\cos\theta+y\sin\theta,\theta)d\theta\,. \tag{8}$$

This method is called filtered back projection.

2.2 Hardware Setup of a Single Source and Detector Gamma Transmission Tomography System

First, we developed a scaled-down version of the single source and detector gamma transmission tomography system. This version enabled us to evaluate how gamma ray CT could be used for a large-scale system such as a packed bed and a distillation column with a 2 m diameter. To characterize gamma ray CT, we constructed a system that gives a degree of freedom with respect to the detector size, the source selection and the aperture size of the collimator.

Table 1. The Specifications of the Lab Scale CT

Resolution/ray-sum	4 mm to 10 mm
Source activity	Cs-137 (20mCi)
Detector	1 inch or 2 inch NaI
Maximum object size	50 cm (in diameter)

2.3 Motion Control and Gamma Ray Detection System

The hardware of the CT system consists of two servo motors, a data logger and a PC. One motor simultaneously moves the source and the detector for a parallel beam scanning, whereas the other motor rotates the scan table at a preset projection angle. The motor is controlled through a driver linked to a data logger for PC control. The driver makes the motor finish a rotation by 12,000 input pulses. The input pulse is generated from the data logger.

The data logger transmits the acquired data to a PC and controls the two servo motor drivers for the rotating and scanning motions. It processes the measured radiation counts as two-dimensional data, the rows and columns which indicate the index s for the location of a detector bin and the projection angle θ, respectively.

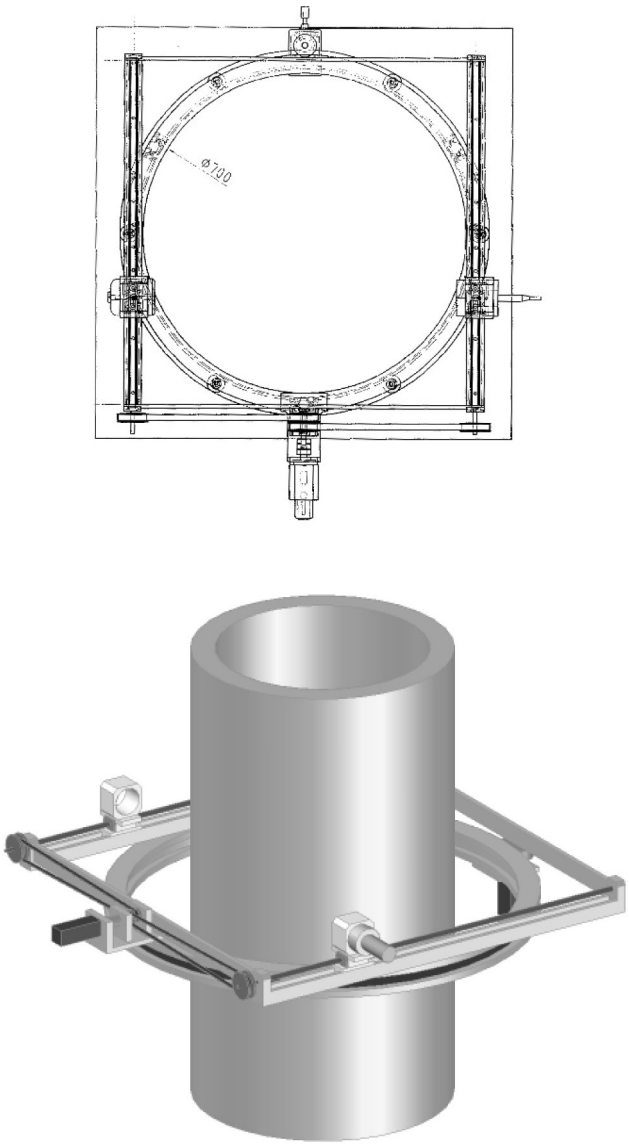

Fig. 4. Hardware Design of the Lab Scale CT

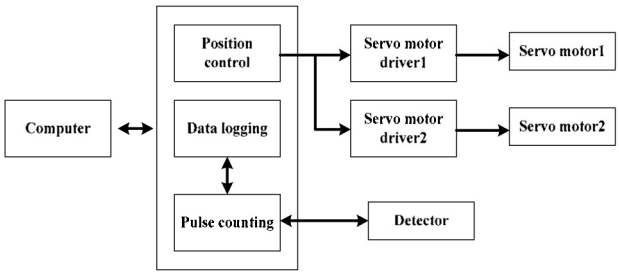

Fig. 5. A Schema of the Gamma CT

Fig. 6. CT Hardware Setup

3. EXPERIMENTAL RESULTS

For the nonspectroscopic counting method, the maximum count rate was 6000 cps with the 20mCi Cs-137 and a 1 inch × 1 inch detector shielded with a 10 mm collimator. The total measurement time took about one and half hours; that is, 30 minutes for the scanning and 60 minutes for the movement of the source and detector. The measurement conditions were based on a 1 second counting time and 32K × 51N, where K is the projection number and N is the number of samples per projection. Figure 8 shows the image from the 64K × 84N data.

In Fig. 8, the sampling interval τ is 6 mm and the highest spatial frequency is $1/2\tau$. By using the sampling theorem and the Nyquist rate, we get a maximum spatial resolution of 12 mm, which enables us to distinguish the image of annual rings.

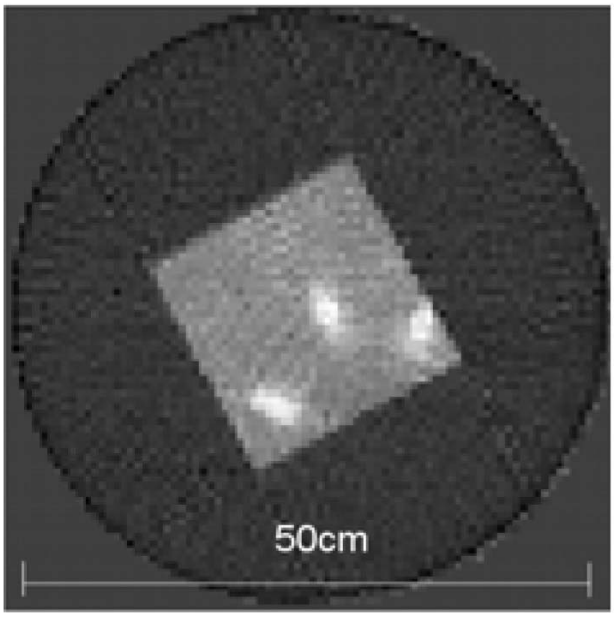

Fig. 8. The Reconstructed Image From the 64K × 84N Data

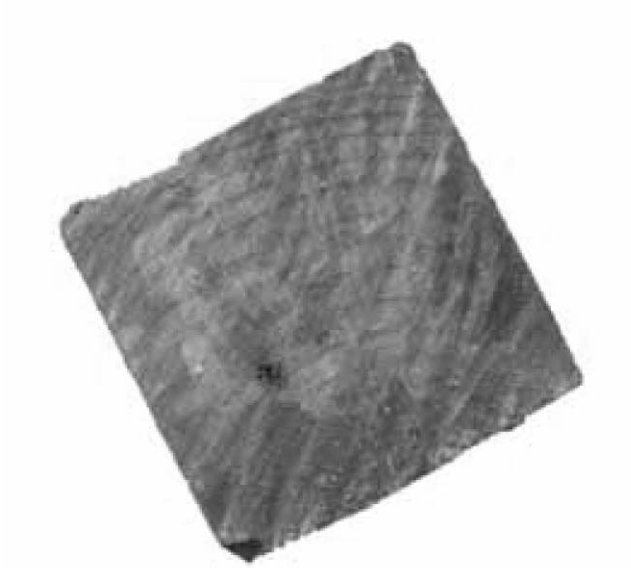

Fig. 7. Wood Sample

3.1 Effects of Statistical Noise

Statistical noise, which is a consequence of random fluctuation in gamma ray photon emissions, causes the ray-sum error to be inversely proportional to the square root of the radiation intensity, namely the number of photons per second. We conducted our experiments with maximum counts: that is, with the value of I_0 being 4400, 6800 and 16,000 for each case. Figure 9 shows that the higher maximum counts produce higher contrast images as a result of the improved signal-to-noise ratio.

3.2 Effects of Collimation

Figure 11(a) and Fig. 11(b) show the μ matrix images as reconstructed from the data obtained with collimation apertures of 5 mm and 10 mm. Figure 10 shows a schema of the detector and source collimator.

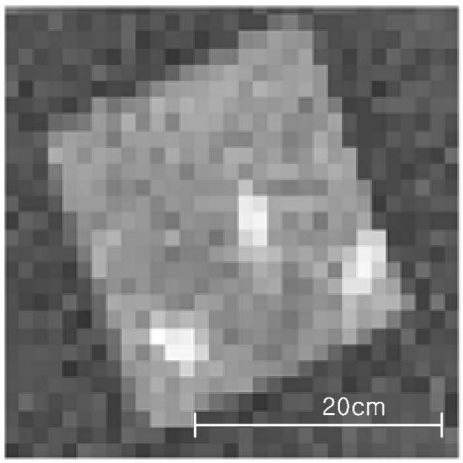

(a) I_0 = 4400 counts (32K×51N)

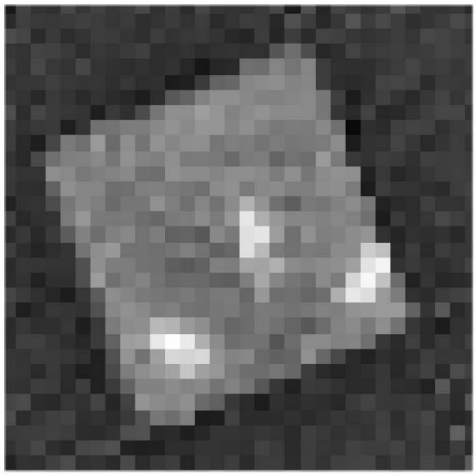

(b) I_0 = 8800 counts (32K×51N)

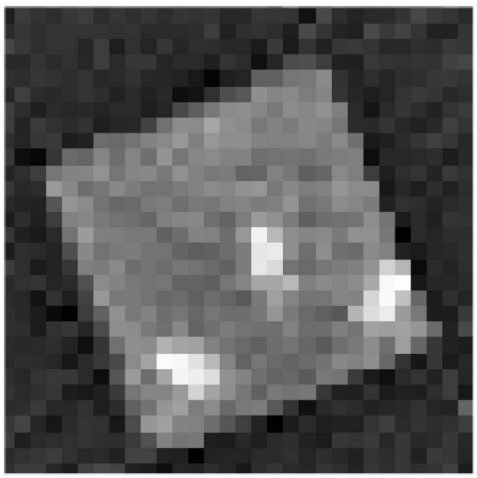

(c) I_0 = 16,000 counts (32K×51N)

Fig. 9. The Effect of the Signal-to-Noise Ratio on the Image Quality

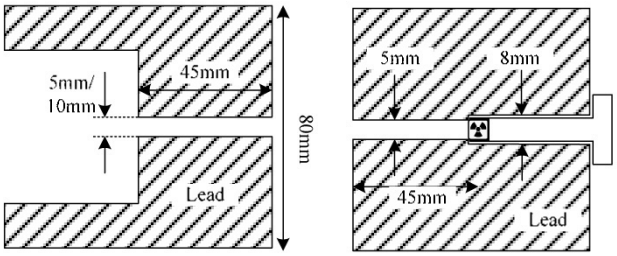

Fig. 10. Detector (left) and Source Collimator (right)

One of the major advantages of narrow beam transmission tomography is the so-called hard field property. This property is capable of producing high quality images, though it decreases the count value and takes a longer time. In contrast, a large collimation diameter produces a fuzzy image but with a faster scanning time. Moreover, in the wood sample in Fig. 11, the enlargement of the aperture from 5 mm to 10 mm barely affects the image quality.

3.3 A Phantom Image Simulation of a Packed Bed Industrial Reactor

We applied gamma ray CT to the phantom of the pipe and bed of an industrial process unit, the size of which was larger than that of a conventional NDT technique. The phantom simulation of a packed bed reactor with air voids was designed on the basis of an example at the Chemical Reaction Engineering Laboratory, Washington University,

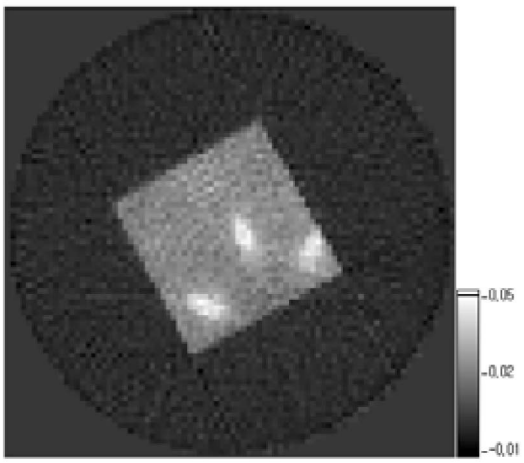

(a) Result of the 5 mm aperture (64K×84N)

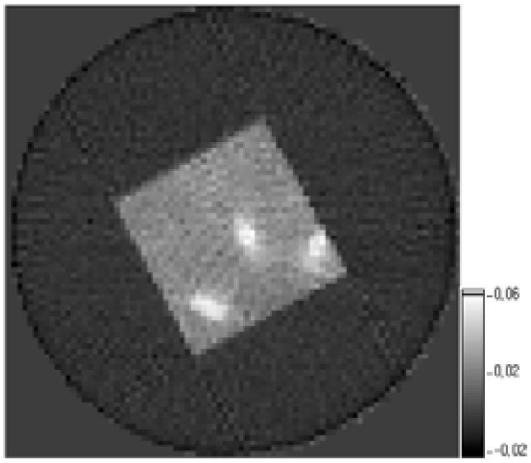

(b) Result of the 10 mm aperture (64K×84N)

Fig. 11. The Images Obtained From Different Sized Apertures

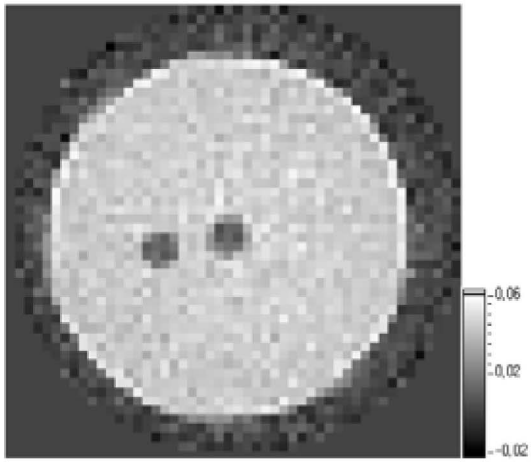

(b) The reconstructed image from the 32K×51N data

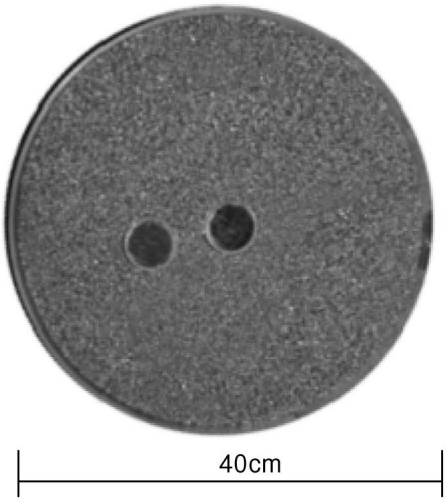

(a) The packed bed phantom filled with polypropylene grains

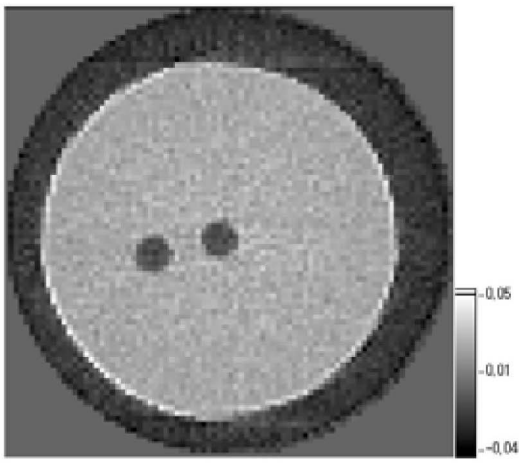

(c) The reconstructed image from the 64K×84N data

Fig. 12. The Gamma CT Experiment on a Phantom of a Packed Bed Reactor

St. Louis [7]. The phantom in Fig. 12(b) and Fig. 12(c) is filled with polypropylene as described in Fig. 12(a). The results of the reconstructed μ matrix image clearly show that voids exist inside the polypropylene bed.

3.4 A Phantom Water-oil-air Layer

In the petrochemical industry, the materials most frequently encountered are oil and plastics. To estimate the contrast of water and oil, we designed the phantom shown in Fig. 13. The image in Fig 13(a) was reconstructed from the following artificial data: the linear attenuation coefficient was 0.0862 cm^{-1} for water and 0.0702 cm^{-1} for oil and the oil-water ratio was 0.815 (μ_oil/μ_water). Figure 13(b) shows the image from the measured data of the water-oil-air layer. The ratio of μcm^{-1} from the results of the reconstruction is 0.812 (μ_oil/μ_water).

Figure 14 compares the reference data and the average reconstructed attenuation value obtained from the gamma-ray CT of a standard object. The results show the operational linearity of an industrial CT system that uses Cs-137.

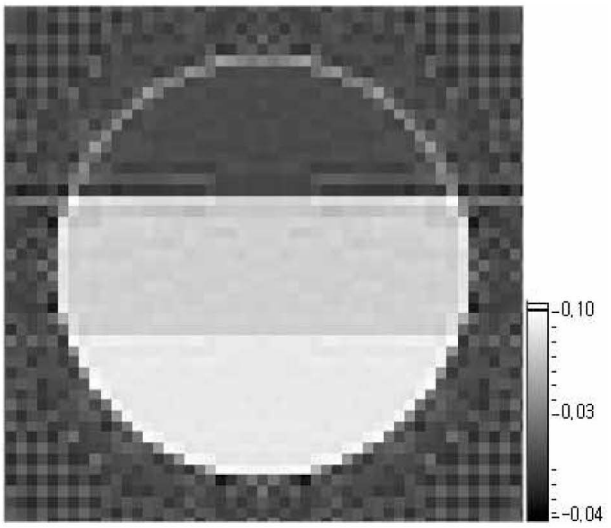

(a) Simulation of the water-oil-air layer (32K×51N)

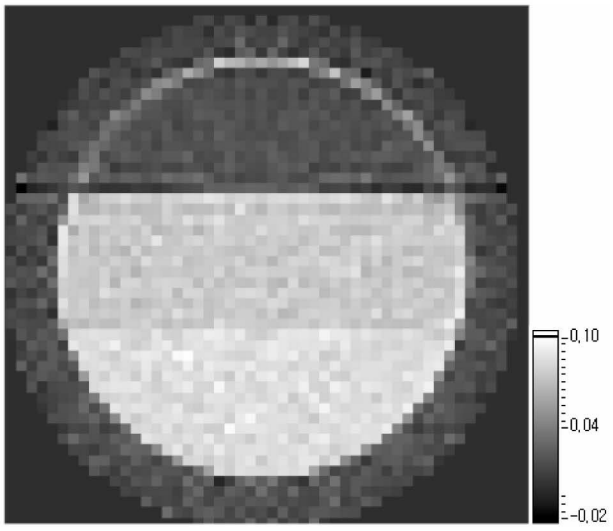

(b) The reconstructed image of the phantom water-oil-gas layer (32K×51N)

Fig. 13. Image Reconstruction of the Water-Oil-Air Layer

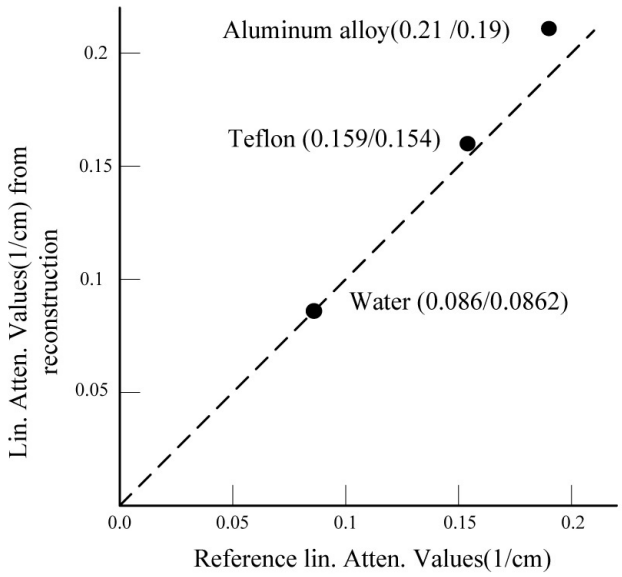

Fig. 14. The Reconstructed Lin. Atten. Values. Vs. the Reference Data of Cs-137

4. CONCLUSION

Although the system is simple and still at an incipient stage, the experimental gamma ray CT image confirms the industrial applicability of the system to process diagnosis. Furthermore, the system can be directly applied to either a packed bed column or a pipe flow. However, the system's geometry and software have room to improve. By adopting a multi-detector or a highly efficient detector, we can reduce the scanning time. We may also consider using a higher energy emitting gamma ray source such as Co-60 for a large-scale system. As for the software that is used for the limited ray-sun, we are currently developing an algebraic reconstruction technique as an alternative to the FBP algorithm.

Future developments of gamma-ray CT will focus on large-scale applications, particularly those that are suitable for practical diagnosis in the petrochemical industry. In a petrochemical plant, more interest should be given to the flow material than to the static system. Hence, for dynamic tomographic images, we should consider using a radioisotope tracer in the emission tomography.

ACKNOWLEDGMENT

This research was conducted under the aegis of the Nuclear R&D Program of the Korean Ministry of Science and Technology.

REFERENCES

[1] Avinash C. Kak, Malcolm Slaney. Principles of Computerized Tomographic Imaging, Electric Copy.IEEE PRESS (1999).
[2] ANIL K. JAIN, Fundamentals of Digital Image Processing p. 431-475, Prentice Hall, Englewood Cliffs (1989).
[3] Nicholas Tsoulfanidis, Measurement and Detection of Radiation, HEMISPHERE PUBLISHING CORPORATION (1981).
[4] Holstad M B, Johansen G A, Jackson P and Eidsnes K S, "Scattered gamma radiation utilised for level measurements

in gravitation separators," *Proc. Int. Conf. New Frontiers of Nuclear Technology: Reactor Physics (PHYSOR 2002)*, Seoul, Korea, Oct. 7-10, 2002.

[5] K S Dyakowski T, Johansen GA, Sankowski D, Mosorov V and Wlodarczyk J, "A dual modality tomography system for imaging gas/solids flows," *The 4th World Congress on Industrial Process Tomography*, Aizu, Japan, Sep. 5-8, 2005.

[6] Johansen G A and Jackson P. Radioisotope gauges for industrial process measurements, John Wiley & Sons, Ltd. (2004).

[7] IAEA, Report of the Second Research Coordination meeting of the Coordinated Research Project on Industrial Process Gamma Tomography,(2005.)